(3) Nose, T.; Chu, B. *Macromolecules* **1979**, *12*, 590.
(4) Chu, B.; Nose, T. *Macromolecules* **1979**, *12*, 599.
(5) Nose, T.; Chu, B. *Macromolecules* **1979**, *12*, 1122.
(6) Chu, B.; Nose, T. *Macromolecules* **1980**, *13*, 122.
(7) Chu, B.; Gulari, Esin; Gulari, Erdogan *Phys. Scr.* **1979**, *19*, 476.
(8) Gulari, Esin; Gulari, Erdogan; Tsunashima, Y.; Chu, B. *J. Chem. Phys.* **1979**, *70*, 3965.
(9) Gulari, Erdogan; Gulari, Esin; Tsunashima, Y.; Chu, B. *Polymer* **1979**, *20*, 347.
(10) de Gennes, P. G. *Macromolecules* **1976**, *9*, 587, 594.
(11) Daoud, M.; Jannink, G. *J. Phys. (Paris)* **1978**, *39*, 331.
(12) Dubois-Violette, E.; de Gennes, P. G. *Physics* **1967**, *3*, 181.
(13) Akcasu, A. Z.; Gurol, H. *J. Polym. Sci., Polym. Phys. Ed.* **1976**, *14*, 1.
(14) Daoust, H.; Rinfret, M. *Can. J. Chem.* **1954**, *32*, 492. Parent, M.; Rinfret, M. *Ibid.* **1955**, *33*, 971.
(15) Horth, A.; Rinfret, M. *J. Am. Chem. Soc.* **1955**, *77*, 503.
(16) Staudinger, H. "Die hochmolekularen organischen Verbindungen"; Springer-Verlag: Berlin, 1932; p 128.
(17) Kotin, L. Ph.D. Thesis, Harvard University, 1960.
(18) (a) Benmouna, M.; Akcasu, Z. *Macromolecules* **1978**, *11*, 1187. (b) Akcasu, Z.; Benmouna, M. *Ibid.* **1978**, *11*, 1193.
(19) Farnoux, B. *Ann. Phys.* **1976**, *1*, 73.
(20) Daoud, M. Thesis, Université de Paris VI, 1977.
(21) Daoud, M.; Cotton, J. P.; Farnoux, B.; Jannink, G.; Sarma, G.; Benoit, H.; Duplessix, R.; Picot, C.; de Gennes, P. G. *Macromolecules* **1975**, *8*, 804.
(22) Chen, F. C.; Yeh, A.; Chu, B. *J. Chem. Phys.* **1977**, *66*, 1290.
(23) Tsunashima, Y.; Moro, K.; Chu, B.; Liu, T. Y. *Biopolymers* **1978**, *17*, 251.
(24) Akcasu, A. Z.; Benmouna, M.; Han, C. C. *Polymer* **1980**, *21*, 866.
(25) Muthukumar, M.; Freed, K. F. *Macromolecules* **1978**, *11*, 843.
(26) Koppel, D. F. *J. Chem. Phys.* **1972**, *57*, 4814.
(27) Chu, B.; Gulari, E. *Macromolecules* **1979**, *12*, 445.
(28) Akcasu, A. Z.; Han, C. C. *Macromolecules* **1979**, *12*, 276.

Static and Dynamical Properties of Polystyrene in Carbon Tetrachloride. 2. Osmotic Pressure and Radius of Gyration in the Dilute, Intermediate, and Semidilute Regions†

B. Chu,* K. Kubota, M.-J. He, and Y.-H. Lin

Chemistry Department, State University of New York at Stony Brook, Long Island, New York 11794. *Received March 25, 1980*

ABSTRACT: Static properties, in terms of the absolute scattered intensity, osmotic compressibility, and radius of gyration, of polystyrene ($\bar{M}_w \sim 1 \times 10^7$) in carbon tetrachloride have been studied from dilute to semidilute polymer concentrations of 0.117 wt % at 18 and 25 °C over a range of scattering angles by means of light scattering intensity meaurements. The main purpose of this study is to strengthen our observation of the intermediate concentration region and to show that both static and dynamical properties exhibit a unique behavior for polymer coils in the neighborhood of an overlap concentration C_1^* before entanglement points become appreciable. Our light scattering intensity results appear to agree with earlier reports on changes of the slope in heat of mixing and density of polymer solutions undergoing a change from the dilute to the semidilute region when the solvents are marginal. We have preliminary evidence to suggest that this unique behavior in the intermediate concentration region depends upon previous thermodynamic history of the polymer solution.

I. Introduction

In the previous article,[1] we made appropriate references to recent experiments and theories related to polymer solutions. Therefore, only specific references will be quoted here. In this companion article, the main purpose is to confirm the observation of an anomalous region between dilute and semidilute solutions and to provide a very qualitative physical picture on this unanticipated behavior for polymer coils in solution based on our preliminary observation of both the static and dynamical properties of a high molecular weight polymer sample (polystyrene, $\bar{M}_w \sim 1 \times 10^7$) in carbon tetrachloride.

II. Brief Theoretical Background

The static properties, such as radius of gyration and osmotic pressure, which can be measured by means of light scattering intensity studies in dilute and semidilute solutions have been discussed in detail elsewhere.[2]

(1) Osmotic Pressure. The osmotic compressibility has the form

$$(\partial\pi/\partial C)_{T,P} = H(\partial n/\partial C)^2_{T,P}CRT/R_c(0) \qquad (1)$$

where $R_c(0)$ [$\equiv R_{vv}(0)$] is the excess Rayleigh ratio due to concentration fluctuations obtained from absolute excess scattered intensity extrapolated to zero scattering angle, using vertically polarized incident and scattered light, $H = 4\pi^2 n^2/N_A\lambda_0^4$, and n, C, N_A, T, P, and R are the refractive index of the solution, the polymer concentration in g/cm^3, Avogadro's number, the absolute temperature, the pressure, and the gas constant, respectively.

For dilute polymer solutions, the chemical potential of the solvent, which is denoted by a subscript 1, is related to the osmotic pressure π by

$$(\mu_1 - \mu_1^\circ) = -\pi V_1 \qquad (2)$$

where V_1 is the partial molar volume of the solvent and $\Delta\mu_1$ ($\equiv\mu_1 - \mu_1^\circ$) represents the chemical potential difference for the solution as a whole. The chemical potential difference can be split into an ideal and an excess term, $\Delta\mu_1 = \Delta\mu_1^{id} + \Delta\mu_1^{ex}$ such that

$$\Delta\mu_1^{ex} = \Delta H_1 - T\Delta S_1^{ex} \qquad (3)$$

where ΔH_1 is the partial molar enthalpy of dilution and ΔS_1^{id} ($=\Delta\mu_1^{id}$) is the ideal partial molar entropy of dilution. At the Θ temperature, $\Delta\mu_1^{ex} = 0$. We shall examine the concentration dependence of $\Delta\mu_1$ from polymer solution to the semidilute solution.

By using a lattice model, Flory[3,4] derived for dilute solutions the following relation for $\Delta\mu_1$:

$$\Delta\mu_1 = RT[\ln(1 - v_2) + (1 - 1/x)v_2 + X_1 v_2^2] \qquad (4)$$

†Work supported by the National Science Foundation Chemistry/Polymer Program (DMR 801652) and the U.S. Army Research Office.

0024-9297/81/2214-0392$01.25/0 © 1981 American Chemical Society

where v_2 is the volume fraction of the polymer, x is the degree of polymerization or the ratio of molar volumes of the polymer and the solvent and defines the size of a polymer species i, and X_1 is a dimensionless quantity which characterizes the interaction energy and is related to the partial molar heat of dilution by

$$\Delta H_1 = RTX_1 v_2^2 \tag{5}$$

in the absence of an entropy contribution. By combining eq 2 and 4, we have

$$\frac{\pi}{C} = \frac{RT}{M} + RT\left(\frac{\bar{v}_2^2}{V_1}\right)\left(\frac{1}{2} - X_1\right)C_1 + RT\left(\frac{\bar{v}_2^3}{3V_1}\right)C^2 + \ldots \tag{6}$$

where $\bar{v}_2$ is the (partial) specific volume of the polymer and M is the polymer molecular weight. The first term on the right side is the ideal, van't Hoff, term. If we take the entropy parameter $\Psi_1 = \Delta S_1^{ex}/Rv_2^2$ and $^1/_2 - X_1 = \Psi_1(1 - \Theta/T)$, eq 6 changes to

$$\frac{\pi}{C} = \frac{RT}{M} + RT\left(\frac{\bar{v}_2^2}{V_1}\right)\Psi_1\left(1 - \frac{\Theta}{T}\right)C + RT\left(\frac{\bar{v}_2^3}{3V_1}\right)C^2 + \ldots \tag{7}$$

indicating explicitly that the second virial coefficient vanishes at the Θ temperature.

In dilute solutions, the segment density throughout the fluid medium is not uniform. To this end, each polymer coil may be regarded as a cloud of polymer segments, with the region between the swarms consisting of solvent molecules. By assuming a Gaussian distribution of segment density of each individual polymer molecule, Flory and Krigbaum[4,5] derived an equation for the osmotic pressure at dilute concentrations

$$\frac{\pi}{C} = \frac{RT}{M} + RT\left(\frac{\bar{v}_2^2}{V_1}\right)\Psi_1\left(1 - \frac{\Theta}{T}\right)F(X)C \tag{8}$$

where

$$X = \left(\frac{3^3}{2^{1/2}\pi^{3/2}}\right)\Psi_1\left(1 - \frac{\Theta}{T}\right)\left(\frac{\bar{v}_2^2}{V_1 N_A}\right)M^2/(\langle r^2\rangle)^{3/2} \tag{9}$$

and

$$F(X) = \frac{8}{3\pi^{1/2}}\int_0^\infty e^{-(y^2+Xe^{-y})^2}y^4\,dy \tag{10}$$

with $\langle r^2\rangle$ being the mean-square end-to-end distance of the random polymer coil. By comparing eq 7 and 8 to the linear C term, we see that the factor $F(X)$ accounts for the inherent nonuniformity of the polymer segment concentration in dilute solutions. $F(X)$ is equal to 1 at the Θ temperature. The better the solvent, the smaller the value of $F(X)$ becomes. As the ideal Θ temperature is approached, eq 7 and 8 become more identical because $F(X)$ approaches unity. Equations 6–10 are not really valid for concentrations close to the semidilute region.

(2) Radius of Gyration. At low scattering angles and very dilute concentrations, we have

$$\frac{HC}{R_{vv}} = \frac{1}{M_w}\left[1 + \frac{16\pi^2 n^2}{3\lambda_0^2}\langle r_g^2(C)\rangle_z^* \sin^2\left(\frac{\theta}{2}\right)\right] + 2A_2C \tag{11}$$

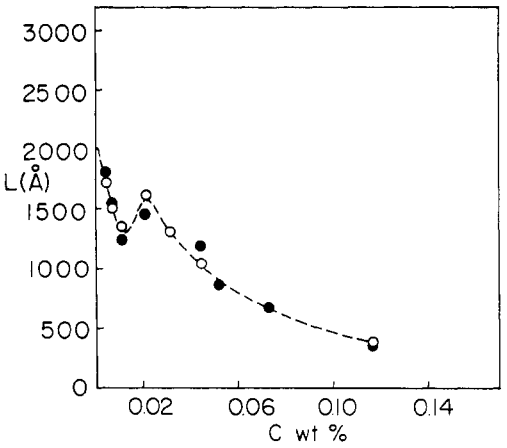

Figure 1. Characteristic length L as a function of concentration at 18 (●) and 25 °C (○).

where A_2 is the second virial coefficient. The apparent radius of gyration, r_g^*, is defined as

$$r_g^{*2} = \langle r_g^2(C)\rangle_z^* = \frac{\langle r_g^2(C)\rangle_z}{(1 + 2A_2CM_w)} = (3\lambda_0^2/16\pi^2n^2)(\text{initial slope})/(\text{intercept}) \tag{12}$$

in a HC/R_{vv} vs. $\sin^2(\theta/2)$ plot

$$\lim_{\theta\to 0}\frac{HC}{R_{vv}} = \frac{1}{M_w} + 2A_2C \tag{13}$$

III. Experimental Methods

The experimental methods have been described elsewhere.[1,2]

IV. Results and Discussion

(1) Radius of Gyration. In dilute solutions [$C \ll C_1^* = M/N_A\rho_s(4/3)\pi r_g^3$) with $r_g^2 \equiv \langle r_g^2(C=0)\rangle$] eq 11–13 are valid. For a high molecular weight polystyrene sample ($M_w \sim 1 \times 10^7$) in a fair solvent (carbon tetrachloride), A_2 is positive.

At higher concentrations, r_g^* is no longer related to r_g according to eq 12. It becomes a measure of the characteristic length (L) in the system[6] with

$$\frac{R_{vv}(0)}{R_{vv}(K)} = 1 + \frac{L^2}{3}K^2 \tag{14}$$

More precisely, L^2 can be identified with r_g^{*2} for $C/C_1^* \ll 1$ and $L^2 \approx \xi^2$ in the semidilute solution region, where ξ denotes a correlation length related to entanglement-point spacings.

Figure 1 shows plots of the characteristic length L as a function of concentration from dilute to semidilute solutions at 18 and 25 °C. In dilute solutions, L decreases with increasing concentration because A_2 is positive. Furthermore, as both 18 and 25 °C represent temperatures far above the Θ temperature for the polystyrene–CCl_4 system, the $\langle r_g^2\rangle_z$ and A_2 values are comparable, with the value at 25 °C being slightly higher than that at 18 °C. The behavior of L between $C \approx 0.01$ and 0.05 wt % is not predicted and represents the first semiquantitative observation on the anomalous characteristic length changes as a function of concentration for a polymer solution in the intermediate concentration region between dilute and semidilute solutions. Such a behavior was not observed for the same polystyrene sample dissolved in *trans*-decalin even at 20 °C above its Θ temperature as shown in Figure 4 of ref 6.

The minimum of r_g^* (or L) occurs at the same concentration as the maximum of the characteristic frequency ($1/\tau$, as shown in Figures 4 and 5 of ref 1). This observation suggests that the anomalous behavior depends on

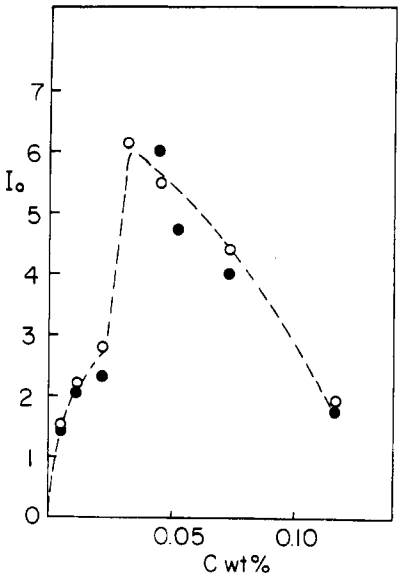

Figure 2. Extrapolated zero scattering angle excess scattered intensity, I_0, as a function of concentration at 18 (●) and 25 °C (○).

the nature of the polymer–solvent systems, the molecular weight, and possibly the temperature. For polystyrene solutions, we know that the polystyrene–*trans*-decalin system[2,6] does not exhibit this anomalous behavior up to 20 °C above its Θ temperature. As the solvent becomes better, e.g., in the polystyrene–CCl_4 system, the strange behavior appears. The appearance of the minimum in L could depend not only on polymer coil size, temperature, and concentration, as denoted by C_1*, but also on excluded-volume effects, in other words, on the interpenetrability and intermolecular interactions of the polymer coils. Perhaps this is one reason that the phenomenon has escaped direct observations in terms of dynamical properties, such as the characteristic frequency, and static properties, such as the apparent radius of gyration, of polymer solutions. The behavior in the semidilute region is as expected.

(2) Osmotic Compressibility and Osmotic Pressure. Figure 2 shows plots of extrapolated zero angle scattered intensity, I_0, as a function of concentration at 18 and 25 °C. The concentration at which the minimum of r_g* (or L) occurs is barely noticeable in the I_0 vs. C plot. The shoulder, however, does not become more prominent at 18 °C than that at 25 °C. The maximum of I_0 coincides with that of L and with the minimum of $1/\tau$ at $C \approx 0.03$ wt %. The shoulder in I_0 represents a new distinct quantity which is different from contributions based on equilibrium thermodynamic considerations. Homogeneous samples at different concentrations, especially those at C = 0.0212 and 0.0316 wt %, were kept at the temperature of measurements (18 or 25 °C) for days to weeks in a constant-temperature bath controlled to ±0.02 °C before transferring them to the light scattering spectrometer. We then repeated the intensity measurements the next day in order to ensure that we had obtained reproducible results in the intermediate concentration region. When the sample was first transferred from the constant-temperature bath to the light scattering spectrometer, whose sample chamber was maintained at the same temperature, large intensity fluctuations sometimes of the order of magnitude of the equilibrium values were observed. We believe that the fluctuations may be caused by small temperature differences between the two thermostats. Further studies on the time dependence of the intensity changes near the intermediate concentration region are in progress.

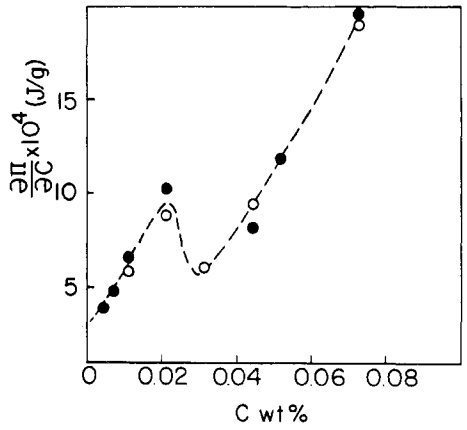

Figure 3. Plots of $(\partial\pi/\partial C)_{T,P}$ vs. concentration at 18 (●) and 25 °C (○).

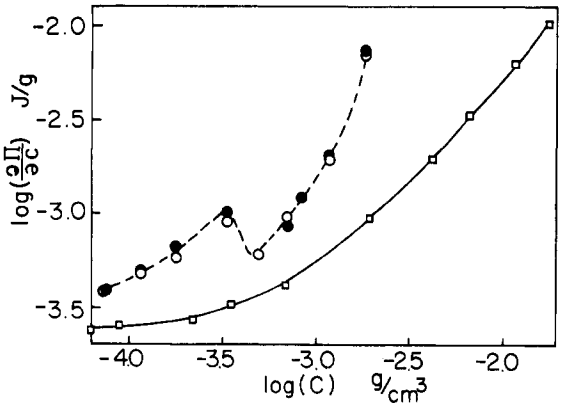

Figure 4. log–log plots of $(\partial\pi/\partial C)_{T,P}$ vs. C (g/cm³) for polystyrene in carbon tetrachloride at 18 (●) and 25 °C (○) in *trans*-decalin[6] at 40 °C (□), where $T - \Theta \approx 20$ °C.

The nature of the intermediate concentration region is further revealed by plots of $(\partial\pi/\partial C)_{T,P}$ as a function of concentration, as shown in Figure 3. We have taken n = 1.468 and 1.463 and $(\partial n/\partial C)_{T,P}$ = 0.149 and 0.155 at 18 and 25 °C, respectively. The minimum in r_g*, the maximum in $1/\tau$, and the shoulder in I_0 occur near $C \sim 0.01$ wt % while the osmotic compressibility, $(\partial\pi/\partial C)_{T,P}$ exhibits a smooth behavior near $C \sim 0.01$ wt %. However, a maximum in $(\partial\pi/\partial C)_{T,P}$ appears near the concentration where the other quantities, L and $1/\tau$, exhibit an inflection point. The concentration where the minimum in $(\partial\pi/\partial C)_{T,P}$ occurs coincides with that where the maximum in I_0 and the minimum in $1/\tau$ occur. In a log–log plot of $(\partial\pi/\partial C)_{T,P}$ vs. C (g/cm³), we have included the osmotic compressibility results of polystyrene in *trans*-decalin[6] measured at 40 °C. The strange behavior is not observed there, as shown in Figure 4. In Figure 1a of ref 6, we noted an anomaly in the $(\partial\pi/\partial C)_{T,P}$ vs. C plot. The anomaly, however, took place near C^* ($=M/N_A\rho_s r_g^3$). The present anomaly takes place near C_1*, which is about 4 times smaller than C^* and is therefore not related to critical phenomena. Furthermore, carbon tetrachloride is a fairly good solvent for polystyrene and $T - \Theta$ is far greater than 20 °C. Similarly, the anomaly in the characteristic length L near C_1* is also absent in the polystyrene–*trans*-decalin system up to $T - \Theta$ = 20 °C.

We can integrate the osmotic compressibility over concentration and estimate the osmotic pressure. Figure 5 shows plots of osmotic pressure π as a function of concentration at 25 °C. Again, we have included the results of the same polymer sample in *trans*-decalin measured at

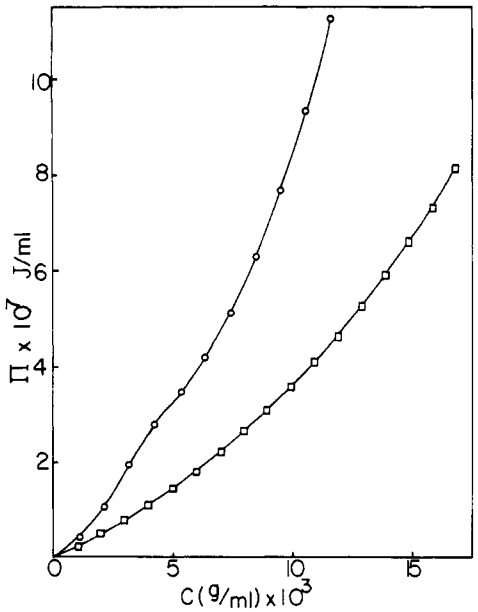

Figure 5. Plots of π vs. C (g/cm^3) of polystyrene in carbon tetrachloride at 25 °C (○) and in *trans*-decalin[6] at 40 °C (□).

40 °C. At infinite dilution, the ideal van't Hoff law holds. At $C < 1 \times 10^{-4}$ g/cm$^3 < C_1$*, the π values are higher at higher temperatures and eq 8 remains valid. At higher concentrations, $C > 5.6 \times 10^{-4}$ g/cm$^3 > C_1$*, the polymer segments are on the average uniformly distributed throughout the solution, and the Flory–Huggins theory[4] again predicts that the osmotic pressure increases with increasing temperature and concentration. In the intermediate concentration region, we have, in fact, observed a bump in the concentration dependence of the osmotic pressure.

V. Conclusions

Static and dynamical properties of polystyrene ($M_w \sim 1 \times 10^7$) in CCl_4 show the existence of an anomalous behavior between dilute and semidilute solutions. Near C_1* we observed a change in the characteristic frequency, a decrease in the characteristic length, and a maximum in $(\partial\pi/\partial C)_{T,P}$. We visualize the polymer coil behavior between concentrations 1×10^{-4} and 5.6×10^{-4} g/cm^3 as individual (though not isolated) coils which are interpenetrable by neighboring coils without appreciable entanglement formation. The behavior is absent in fluid mixtures of small molecules, in polymer solutions under Θ conditions, and in a good solvent. It has been compared with the change of slope in heats of mixing and density of polymer solutions[7,8] in the intermediate concentration range and has been suggested incorrectly as a form of pseudotransition behavior.[9] The details of the metastable state in the intermediate concentration region will be reported in a separate article.

References and Notes

(1) Lin, Y.-H.; Chu, B. *Macromolecules*, preceding paper in this issue.
(2) Nose, T.; Chu, B. *Macromolecules* **1979**, *12*, 590.
(3) Flory, P. J. *J. Chem. Phys.* **1942**, *10*, 51.
(4) Flory, P. J. "Principles of Polymer Chemistry"; Cornell University Press: Ithaca, N.Y., 1953.
(5) Flory, P. J.; Krigbaum, W. R. *J. Chem. Phys.* **1950**, *18*, 1086. Flory, P. J. *Ibid.* **1949**, *17*, 1347.
(6) Chu, B.; Nose, T. *Macromolecules* **1980**, *13*, 122.
(7) Daoust, H.; Rinfret, M. *Can. J. Chem.* **1954**, *32*, 492.
(8) Parent, M.; Rinfret, M. *Can. J. Chem.* **1955**, *33*, 971.
(9) Chu, B.; Lin, Y.-H.; DiNapoli, A.; Nose, T.; Kuwahara, N. *Ferroelectrics* **1980**, *30*, 255.

Study of Thermal Polymerization of Styrene by Raman Scattering

B. Chu,* G. Fytas,† and G. Zalczer‡

Department of Chemistry, State University of New York at Stony Brook, Long Island, New York 11794. *Received May 22, 1980*

ABSTRACT: We present a new method for studying polymerization kinetics based on Raman scattering. Our method has selectivity, is reliable and easy to apply, can be automated, and is insensitive to most spurious phenomena. We demonstrate this method by a study of the thermal polymerization of styrene at 60, 75, and 90 °C.

Introduction

The thermal polymerization of styrene has recently been the subject of several studies by light-beating spectroscopy (polarized[1] and depolarized[2]), interferometry (polarized[3] and depolarized[4]), and NMR.[5] We present here a new method based on Raman scattering. Our method has selectivity, is reliable and easy to apply, can be automated, and involves little external calibration. We emphasize that, since polymerization involves changes in chemical bonds which can usually be observed through Raman lines, this technique should be applicable to almost any polymerization process.

† On a leave of absence from the University of Bielefeld, Faculty of Chemistry PC1, 48 Bielefeld 1, West Germany.
‡ On a leave of absence from the Commissariat à l'Energie Atomique, Centre d'Etudes Nucléaires de Saclay, SPSRM, BP 2, 91190 Gif-s/Yvette, France.

Principle and Calibration

The principle of the method is to record Raman spectra from the sample at different stages of polymerization. In a polymerization reaction some portion of the molecular structure of interest usually remains unchanged. The corresponding Raman-active lines are present throughout the process and can be used as standards to calibrate the intensity of other lines, while those related specifically to the monomer vanish and those related to the polymer grow. Monitoring a ratio of intensities makes the measurement insensitive to laser power fluctuations or sample turbidity. Therefore, the method is reliable even in unfavorable conditions. In particular, applications of the method for studying copolymerization processes should be a worthwhile extension.

The first step is to measure Raman spectra of the monomer and of the polymer and to select the useful lines. When many Raman peaks are present, some of this in-

0024-9297/81/2214-0395$01.25/0 © 1981 American Chemical Society